

# Structural and Mutational Analysis of Affinity-Inert Contact Residues at the Growth Hormone–Receptor Interface

Kenneth H. Pearce, Jr., Mark H. Ultsch, Robert F. Kelley, Abraham M. de Vos,\* and James A. Wells\*

Department of Protein Engineering, Genentech, Inc., 460 Point San Bruno Boulevard, South San Francisco, California 94080

Received March 1, 1996; Revised Manuscript Received May 1, 1996<sup>®</sup>

**ABSTRACT:** Mutational studies have shown that over two-thirds of the contact side chains at the human growth hormone (hGH)–receptor interface have little or no impact on binding affinity when converted to alanine [Cunningham, B. C., & Wells, J. A. (1993) *J. Mol. Biol.* 234, 554–563; Clackson, T., & Wells, J. A. (1995) *Science* 267, 383–386]. Herein, three of the most buried, yet functionally inert, residues on hGH (F25, Y42, and Q46) have been simultaneously mutated to alanine. Binding kinetics of the triple-alanine mutant shows that neither association nor dissociation rates are significantly affected and only slight, local disorder is seen in the crystal structure. However, large and compensating changes were observed in the enthalpy and entropy of binding as determined by isothermal titration calorimetry. The triple-alanine mutant bound with a more favorable enthalpy ( $\Delta H = -12.2 \pm 0.7$  kcal/mol) and corresponding less favorable entropy [ $\Delta S = -2.3 \pm 2.4$  cal/(mol·K)] compared to the wild-type interaction [ $\Delta H = -9.4 \pm 0.3$  kcal/mol;  $\Delta S = 7.7 \pm 1.2$  cal/(mol·K)]. Dissection of the triple-alanine mutant into the single F25A and double Y42A/Q46A mutants showed that the more favorable enthalpy was derived from the removal of the F25 side chain on helix-1 of the hormone. The  $\Delta C_p$  values for both the triple-alanine mutant [ $-927 \pm 10$  cal/(mol·K)] and the individual mutants were significantly more negative than the  $\Delta C_p$  for the wild-type interaction [ $-767 \pm 34$  cal/(mol·K)]. Such negative  $\Delta C_p$  values are consistent with the proposal that the hydrophobic effect is the primary contributor to the free energy of binding at this protein–protein interface. These results show that multiple-alanine mutations at contact residues may not affect binding kinetics, affinity, or global structure; however, they can produce local structural changes and can cause large compensating effects on the heat and entropy of binding. These studies emphasize that one cannot infer binding free energy from the existence of contacts alone and further support the notion that only a small set of contacts are crucial for the human growth hormone–receptor interaction.

Protein–protein complexes play fundamental roles in many biological processes such as hormone–receptor interactions, enzyme regulation, immune recognition, signal transduction, transcription regulation, and cell motility. To elucidate how molecular recognition processes govern complex biological systems, it is necessary to better understand the noncovalent forces that drive protein–protein interactions. The complex between human growth hormone (hGH)<sup>1</sup> and two molecules of the extracellular domain of its receptor (called the hGHbp) is one of the best characterized protein–protein complexes [for review see Wells and De Vos (1996)]. X-ray crystallography has identified the molecular contacts between the two sites on hGH (called site 1 and site 2) and the two bound hGHbp's (De Vos et al., 1992; Ultsch & De Vos, 1993). Virtually all the contacts at these interfaces are made by side chains.

Alanine-scanning mutagenesis of the site 1 interface between hGH and its first bound hGHbp probed the energetic importance of these contact side chains from both hormone

and receptor sides (Cunningham & Wells, 1989, 1993; Clackson & Wells, 1995). These studies revealed that only a small set of the contact side chains are critical for binding (Figure 1). For example, three critical residues at site 1 on hGH (R64, K172, and R178), which make between 7 and 26 van der Waals contacts to the hGHbp using side chain atoms beyond the  $\beta$ -carbon, reduced binding affinity by 16–60-fold when converted to alanine (Table 1). In contrast, three other contact residues (F25, Y42, and Q46), which make between 6 and 27 van der Waals contacts, had no significant impact on binding affinity when converted to alanine. These three inert contact residues are among the most buried residues at the site 1 interface; together these nonfunctional residues account for 16% of the 1300 Å<sup>2</sup> surface area buried when hGH binds the first hGHbp.

The primary motivation for this investigation was to study the mutational effects at these affinity-inert contact residues (F25, Y42, and Q46) by analysis of the structure of the 1:1 complex, binding kinetics, and thermodynamics. Remarkably little change was found in the binding affinity, kinetics, or global structure of the complex. However, local changes in structure were observed, as well as large and compensating changes in the enthalpy and entropy of the reaction. The central core of critical contact residues (“the hot spot”) appears to function independently of these peripheral, inert contacts. The results presented herein lend further support to the possibility that building small molecule mimics of such

\* To whom correspondence should be addressed.

<sup>®</sup> Abstract published in *Advance ACS Abstracts*, July 15, 1996.

<sup>1</sup> Abbreviations: hGH, human growth hormone; hGHbp, soluble, extracellular domain of the human growth hormone receptor; PBS, phosphate-buffered saline; RU, refractive index unit. Mutant proteins are named with the single-letter code for the wild-type residue, followed by the amino acid position and the single-letter code for the mutation residue. Multiple mutants are indicated by the single site changes separated by slash marks.

compact functional regions may provide a rational approach to drug design at large protein–protein interfaces.

## MATERIALS AND METHODS

Site-directed mutagenesis and expression of hGH variants were performed as described (Cunningham & Wells, 1989). All hGH proteins were purified to homogeneity by gel filtration (Sephacryl-100 HR; Pharmacia Biotech, Inc.) and hydrophobic interaction chromatography (Toyopearl phenyl 650M; TosohHaas). Mass spectrometry was used to verify the mass of all variant proteins. The hGHbp was expressed and purified as described (Ultsch & De Vos, 1993). Concentrations of proteins were determined by OD<sub>280</sub> using  $\epsilon_{280} = 19\,560, 16\,942, 19\,937, 16\,118, \text{ and } 64\,345 \text{ (M}^{-1}\cdot\text{cm}^{-1}\text{)}$  for G120R, F25A/Y42A/Q46A/G120R, F25A/G120R, Y42A/Q46A/G120R, and hGHbp, respectively, as calculated from quantitative amino acid analysis.

**Kinetic and Equilibrium Binding Analysis.** Association rates ( $k_{\text{on}}$ ), dissociation rates ( $k_{\text{off}}$ ), and equilibrium binding constants ( $K_d$ ) were determined using surface plasmon resonance (Karlsson et al., 1991) on a Pharmacia BIAcore instrument. Introduction of a cysteine residue (S201C) into hGHbp allowed for uniform immobilization of receptor to the sensor chip as described (Cunningham & Wells, 1993). Typically, S201C hGHbp was reacted with the activated sensor chip to yield between 1000 and 1200 refractive index units (RU). Dissociation rates were measured by passing 35  $\mu\text{L}$  of either 2  $\mu\text{M}$ , 5  $\mu\text{M}$ , or 10  $\mu\text{M}$  hGH in phosphate-buffered saline (PBS: 10 mM sodium phosphate, 137 mM NaCl, 2.7 mM KCl, pH 7.2) with 0.05% Tween-20 at a flow rate of 20  $\mu\text{L}/\text{min}$  over the sensor chip; after the injection, the decrease in RU's was monitored with time. Association rates were determined from the concentration dependence of the binding profiles for various hGH solutions. Typically, 1.25  $\mu\text{M}$  solutions of ligand were serially diluted (2-fold) six times, and 35  $\mu\text{L}$  was injected with flow rates of 20  $\mu\text{L}/\text{min}$ . Sensor chips were regenerated as described (Cunningham & Wells, 1993). Binding profiles were analyzed by nonlinear regression using a simple monovalent binding model (BIAevaluation version 2.0; Pharmacia Kinetics). Equilibrium dissociation constants were calculated by  $K_d = k_{\text{off}}/k_{\text{on}}$ .

**Structure Determination by X-ray Crystallography.** The complex was formed by adding a 1:1 ratio of the hGH variant and hGHbp and purified over a size exclusion column. Crystals of the complex were grown as described (Ultsch & De Vos, 1993; De Vos and Ultsch, in preparation), in space group  $P4_32_12$ , with cell parameters  $a = 66.34 \text{ \AA}$  and  $c = 227.3 \text{ \AA}$  and contained one complex per asymmetric unit. The crystals diffracted anisotropically, to about 2.7  $\text{\AA}$  in the  $a^*, b^*$  plane but to much higher resolution along  $c^*$ . Diffraction data were collected at 100 K from a flash-frozen crystal using a Mar Research imaging plate mounted on a Rigaku RU200 X-ray generator operated at 45 kV and 90 mA, with graphite-monochromated Cu K $\alpha$  radiation. Data were processed with XDS (Kabsch, 1988). The final data set was 98% complete to 2.69  $\text{\AA}$  resolution, comprising a total of 14 559 unique reflections (3.9-fold redundancy;  $R_{\text{merge}} = 4.2\%$ ). The starting model for refinement consisted of the 2.6  $\text{\AA}$  structure of the complex between the G120R mutant of hGH and hGHbp, refined to an  $R$ -value of 0.187 (De Vos and Ultsch, in preparation). Refinement was carried

out using X-PLOR (Brünger, 1992) and the Engh and Huber parameter set (Engh & Huber, 1991); no  $\sigma$  cutoff was applied, but the data were corrected for anisotropy (yielding a 23  $\text{\AA}^2$  difference between the  $a^*, b^*$ , and  $c^*$  directions). Rigid-body refinement of the model gave a crystallographic  $R$ -value of 0.35 (data between 10 and 2.7  $\text{\AA}$  resolution), and cycles of rebuilding using FRODO (Jones, 1978) and positional refinement and refinement of individual temperature factors resulted in a final  $R$ -value of 0.229 (all 13 775 reflections between 8 and 2.7  $\text{\AA}$  resolution). The final model consists of residues 2–45, 52–129, 136–148, and 156–189 of hGH and residues 33–52, 61–72, and 79–237 of the receptor, with 17 water molecules. The stereochemistry of the protein molecules is characterized by rms deviations from ideality of 0.013  $\text{\AA}$  and 1.8° in bond lengths and angles, respectively, and the average  $B$ -factor for all 2890 non-hydrogen atoms is 36.9  $\text{\AA}^2$  (the rms  $B$ -factor difference between bonded atoms is 2.4  $\text{\AA}^2$ ).

**Isothermal Titration Calorimetry.** Measurement of the enthalpy change ( $\Delta H$ ) for the variant hGH–hGHbp interactions was performed on a MicroCal OMEGA titration calorimeter (Wiseman et al., 1989; MicroCal Inc., Northampton, MA) coupled with a nanovolt preamplifier. Protein solutions were dialyzed exhaustively against PBS, passed through a 0.2  $\mu\text{m}$  filter, and degassed before use. Experiments were performed at  $26.2 \pm 0.2, 29.1 \pm 0.2, 34.4 \pm 0.2$ , and  $38.8 \pm 2^\circ\text{C}$ . The sample cell (1.394 mL) was loaded with hGHbp solution (typically between 5 and 15  $\mu\text{M}$ ). While being stirred at 400 rpm, the system was allowed to equilibrate to an rms noise value of 0.002  $\mu\text{cal/s}$  before beginning the injections of hGH variants. The injection syringe (43.2  $\mu\text{L}/\text{in.}$ ) was filled with hGH variant solutions (between 150 and 300  $\mu\text{M}$ ), and a number of injections (typically 2–3 nmol each) were made. Injections were continued beyond saturation of the hGHbp to allow for determination of heats of ligand dilution. Calorimetric data were analyzed by integration of resultant peaks (version 2.9; MicroCal Software, Inc.), and heats of dilution were subtracted from heats of binding to yield  $\Delta H_{\text{assoc}}$ . The calorimeter was calibrated electrically using the provided software and periodically by titration with hydrochloric acid.

## RESULTS AND DISCUSSION

The three affinity-inert contact residues, F25, Y42, and Q46, lie in the periphery of the central cluster of functionally important residues that form site 1 on hGH for binding the first hGHbp (Figure 1). F25 is located in the middle of helix-1; Y42 and Q46 are in the first minihelical segment that follows helix-1. These three residues were mutated to alanine and combined with an additional mutation in site 2, G120R (Fuh et al., 1992; Cunningham & Wells, 1993). The G120R prevents the hormone from complexing a second molecule of the hGHbp, thus ensuring that the kinetic and thermodynamic effects are confined to binding events at site 1 alone. Control experiments have shown that G120R has no significant effect on the binding kinetics or affinity at site 1 relative to wild-type hGH (Cunningham & Wells, 1993). Finally, the G120R allows crystallization of the triple-alanine mutant as a 1:1 complex with the hGHbp (Ultsch & De Vos, 1993).

*The Three Alanine Mutations Cause Little Change in the Structure of the 1:1 Mutant hGH–hGHbp Complex.* The

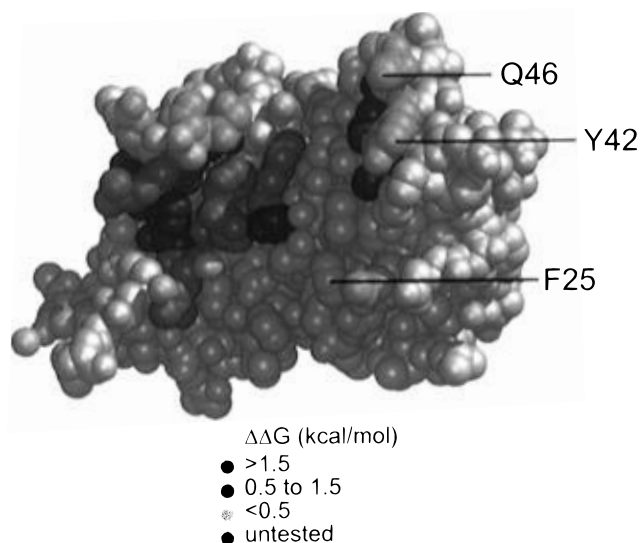


FIGURE 1: Space-filling model of the hGH site 1 interface. Colors reflect the functional significance of receptor contact residues. Light blue residues indicate  $\Delta\Delta G(\text{mut-wt}) < 0.5$  kcal/mol; dark blue residues indicate  $\Delta\Delta G(\text{mut-wt}) 0.5\text{--}1.5$  kcal/mol; red residues are most important,  $\Delta\Delta G(\text{mut-wt}) > 1.5$  kcal/mol [data from Cunningham and Wells (1993)]. Yellow spheres show positions of ordered water molecules that reside at the hGH–hGHbp interface (coordinates from A. M. De Vos, unpublished results). Residues chosen for mutation to alanine are labeled. All structure figures were produced using the MIDAS molecular graphics package (Ferrin et al., 1988).

structure of the F25A/Y42A/Q46A/G120R hGH–hGHbp complex was determined at 2.7 Å resolution and refined to a crystallographic *R*-value of 0.229. The mutant complex is virtually superimposable with that of the 1:1 G120R hGH–hGHbp complex (Figure 2). The average rms difference in coordinates for 237 common C $\alpha$  atoms in the triple-alanine mutant and the G120R 1:1 complex is 0.44 Å and is comparable to that between the 1:1 and 1:2 hGH–hGHbp complexes (A. De Vos and M. Ultsch, unpublished results). This small difference reflects random error in the coordinates of the final structure.

The structures of the triple-alanine mutant and G120R 1:1 complexes are virtually superimposable in the helix-1 region of hGH containing the F25A mutation (Figure 3A). Except for the missing phenyl ring and an ordered water molecule 4.8 Å from the  $\beta$ -carbon of F25, the positions of helix-1 and side chains therein are virtually the same for the triple-alanine mutant and the G120R hGH. Although the missing phenyl ring deletes six van der Waals contacts (i.e., atom–atom distances  $\leq 4.4$  Å) with the receptor, the receptor residues show only slight changes in conformation between the two complexes. In fact, similar differences in conformation are seen in this region around G220 of the receptor for the wild-type 1:1 and 1:2 complexes (A. De Vos, unpublished observations). Thus, these slight changes are not attributable to the mutation of F25 to alanine.

Unlike the well-defined structure for helix-1 of the triple-alanine mutant, the minihelical region (residues 38–47) is not well ordered in the electron density map, and therefore most of this region could not be accurately modeled (Figure 3B). This apparently reflects disorder in this segment that is specific for the Y42A/Q46A mutations because the minihelix is ordered in the 1:1 G120R complex (De Vos & Ultsch, in preparation). Generally, the minihelix appears to be a metastable structure; it is often seen in different

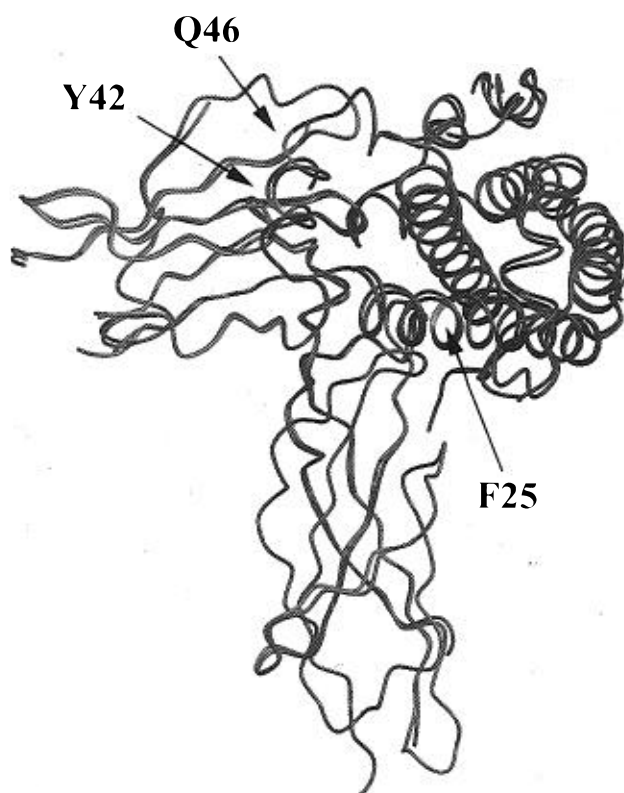


FIGURE 2: Alignment of the backbone structures for the G120R hGH–hGHbp and F25A/Y42A/Q46A/G120R hGH–hGHbp complexes. The 1:1 complexes of G120R (dark red) and F25A/Y42A/Q46A/G120R (dark blue) with hGHbp (light red and light blue, respectively) were superimposed using secondary structural elements for alignment and yielded an rms difference of 0.44 Å among 237 common C $\alpha$  atoms.

conformations in different structures. For example, in the original structure of uncomplexed porcine GH (70% sequence identity to hGH) this region is apparently not helical (Abdel-Meguid et al., 1987); however, it is partially helical in the uncomplexed structure of human placental lactogen (85% sequence identity to hGH) (W. Somers, L. Pelletier, A. De Vos, and A. Kossiakoff, unpublished results). For an affinity-optimized variant of hGH (Lowman & Wells, 1993), which contains four mutations in this helix, the minihelix is present in the free hormone (Ultsch et al., 1994) but exists in an extended, partially unwound form when complexed to the hGHbp (C. Schiffer, W. Somers, M. Ultsch, A. De Vos, and A. Kossiakoff, unpublished results).

The Y42A/Q46A mutations delete a total of 37 atom–atom contacts ( $\leq 4.4$  Å) with the receptor, among them being the loss of a hydrogen bond (3.0 Å) between Q46 and E120 on the hGHbp. This interaction does not appear to contribute significantly to receptor binding because binding affinity is practically unchanged for the Q46A mutation (Table 1). Despite the absence of these contacts, the receptor contact residues in this region are not substantially changed compared to the G120R 1:1 structure (Figure 3B). One exception is the loop between receptor residues 72 and 79 which is disordered in the mutant complex. Like the first minihelical region of hGH, this receptor loop is seen to be flexible in all hGH crystal structures. Thus, while the structural changes in the hGH minihelix and receptor loop are clearly the largest observed between the triple-alanine mutant and G120R 1:1 complex, these changes appear in regions that are prone to conformational variation.

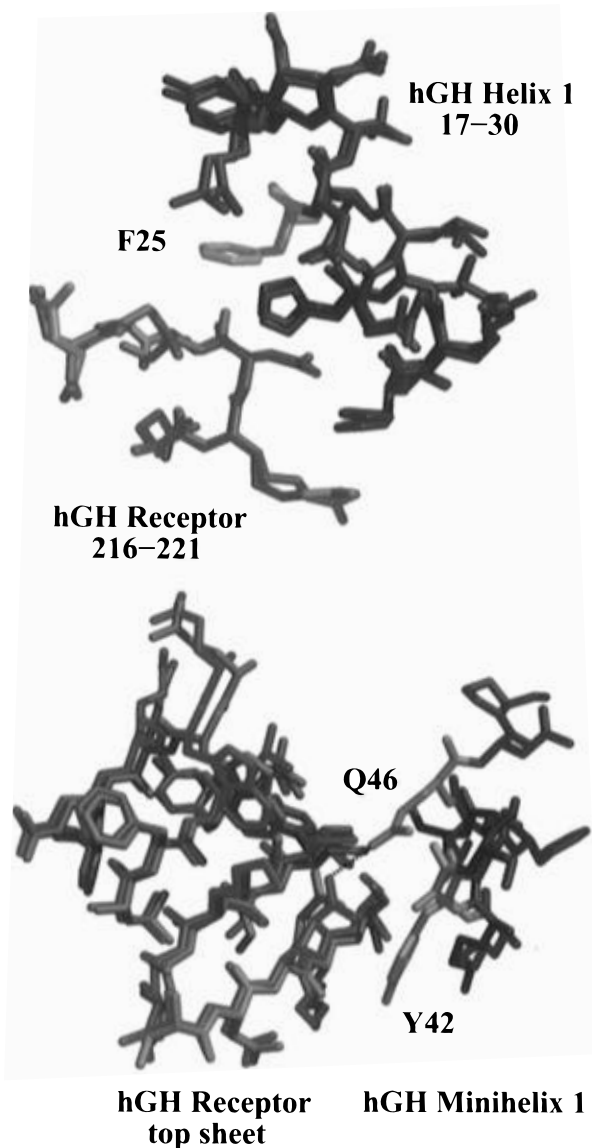


FIGURE 3: Close-up of the contact regions of G102R-hGHbp and F25A/Y42A/Q46A/G120R-hGHbp in areas near the mutated residues. The residues of the G120R hGH-hGHbp complex and the F25A/Y42A/Q46A/G120R hGH-hGHbp complex are shown in red shades and blue shades, respectively. Panel A (top): Shown are the regions surrounding the F25A mutation on helix-1 and the corresponding receptor contact residues. Panel B (bottom): The N-terminal  $\beta$ -sheet domain of the receptor is shown in contact with mini-helical residues 40–47 for the G120R complex. Not all residues in the minihelix region of the triple-alanine hGH complex were visible in the crystal structure. The dotted line represents a 3.0 Å H-bond between E120 and Q46 in the G120R hGH-hGHbp complex.

*The Three Alanine Mutations Cause Little Change in Binding Kinetics or Affinity.* The kinetics of binding of hGH variants to hGHbp was measured using a BIAcore instrument (Pharmacia). Within a microfluidic flow cell, the BIAcore monitors soluble protein binding to an immobilized ligand by using changes in surface plasmon resonance that are caused by a change in solution refractive index near a planar surface. The hGHbp was specifically immobilized to the sensor chip's dextran matrix via an engineered thiol (S201C) to provide uniform receptor orientation and to further prevent dimer formation of the hGHbp in the flow cell (Cunningham & Wells, 1993). The association rates were determined from the concentration dependence on the rate of association of

Table 1: Comparison of Surface Area Buried to Effect on Affinity (Alanine Mutation) for Residues at the hGH-hGHbp Interface

residue	$K_d(\text{mut})/K_d(\text{wt})^a$	reduction in VDW contacts ( $\leq 4.4$ Å) <sup>b</sup>	decrease in solvent-accessible area (Å <sup>2</sup> ) upon binding for wt residue side chain <sup>b</sup>
R64A	16	26	124
K172A	30	12	28
R178A	60	7	66
F25A	0.5	6	52
Y42A	1.4	27	82
Q46A	1.2	10	68

<sup>a</sup> Functional data were taken from Cunningham and Wells (1993).

<sup>b</sup> Values were determined using the coordinates of the 1:1 hGH G120R-hGHbp complex (A. De Vos and M. Ultsch, unpublished results). The reduction in number of van der Waals contacts is simply defined as the loss of atom-atom contacts ( $\leq 4.4$  Å) when atoms beyond the  $\beta$ -carbon of a side chain are removed. Solvent accessibility upon complex formation was calculated according to methods of Lee and Richards (1971) using a probe radius of 1.4 Å. The total surface area of the hormone buried by receptor is approximately 1300 Å<sup>2</sup>.

Table 2: Kinetic and Equilibrium Constants for hGH Variant Binding to hGHbp<sup>a</sup>

hGH variant	$k_{\text{off}} \times 10^{-4}$ (s <sup>-1</sup> )	$k_{\text{on}} \times 10^5$ (M <sup>-1</sup> s <sup>-1</sup> )	$K_d$ (nM)
G120R	4.9 ( $\pm 0.5$ )	1.7 ( $\pm 0.3$ )	2.9 ( $\pm 0.6$ )
F25A/Y42A/Q46A/G120R	5.0 ( $\pm 0.2$ )	1.2 ( $\pm 0.3$ )	4.0 ( $\pm 0.9$ )
F25A/G120R	2.8 ( $\pm 0.1$ )	1.9 ( $\pm 0.1$ )	1.4 ( $\pm 0.1$ )
Y42A/Q46A/G120R	8.5 ( $\pm 0.1$ )	1.8 ( $\pm 0.1$ )	4.6 ( $\pm 0.3$ )

<sup>a</sup> Dissociation rates ( $k_{\text{off}}$ ) and association rates ( $k_{\text{on}}$ ) were determined by BIAcore analysis at room temperature as described in Materials and Methods. Equilibrium binding constants were determined by  $K_d = k_{\text{off}}/k_{\text{on}}$ . Errors represent the standard deviation from between two and seven individual measurements.

the hGH variants. As seen in Table 2, none of the mutations caused significant changes in the association rate. This is consistent with previous findings showing that alanine mutations at any contact residue (whether important for affinity or not) had little effect on the on-rate (Cunningham & Wells, 1993).

Generally, off-rate values are more influenced by mutation of interfacial residues; previous work has shown that when functionally important residues at the hGH-hGHbp interface were converted to alanine, off-rate values increased up to 30-fold (Cunningham & Wells, 1993). However, when the three buried hGH residues chosen for the present study were mutated to form the triple-alanine variant, the off-rate was virtually unchanged compared to the G120R control (Table 2). Dissection of the triple-alanine mutant into the individual helix-1 (F25A) and minihelix-1 (Y42A/Q46A) mutants showed slight and compensating effects on the off-rate. The F25A mutant demonstrated about a 2-fold slower dissociation, whereas the Y42A/Q46A double mutant caused about a 2-fold faster dissociation rate. The effects on the equilibrium constant (calculated from  $K_d = k_{\text{off}}/k_{\text{on}}$ ) simply reflected the small effects observed for the off-rate.

*The Three Alanine Mutations Cause Large Compensatory Changes in the Enthalpy and Entropy of Binding.* The free energies of binding ( $\Delta G_{\text{assoc}}$ ) for these variants of hGH, calculated from the equilibrium constant, were all approximately -12 kcal/mol (Table 3). To dissect how much of  $\Delta G_{\text{assoc}}$  was attributable to a change in the enthalpy of binding ( $\Delta H$ ) or entropy of binding ( $\Delta S$ ), isothermal titration calorimetry was used to directly measure the  $\Delta H$  values for

Table 3: Thermodynamic Parameters for hGH Variant Binding to hGHbp ( $26.2 \pm 0.1$  °C)<sup>a</sup>

hGH variant	$\Delta G^b$ (kcal/mol)	$\Delta H$ (kcal/mol)	$\Delta S$ [cal/(mol·K)]	$\Delta C_p^c$ [(cal/(mol·K))]
G120R	$-11.7 \pm 0.2$	$-9.4 \pm 0.3$	$7.7 \pm 1.2$	$-767 \pm 34$
F25A/Y42A/Q46A/G120R	$-11.5 \pm 0.2$	$-12.2 \pm 0.7$	$-2.3 \pm 2.4$	$-927 \pm 10$
F25A/G120R	$-12.1 \pm 0.1$	$-12.2 \pm 0.8$	$-0.3 \pm 2.7$	$-956 \pm 69$
Y42A/Q46A/G120R	$-11.4 \pm 0.1$	$-9.8 \pm 1.0$	$5.3 \pm 3.4$	$-962 \pm 74$

<sup>a</sup> Changes in enthalpy ( $\Delta H$ ) were measured by isothermal titration calorimetry as described in Materials and Methods. Values represent the average of between 4 and 13 ligand injections, using two independent ligand and receptor preparations (with the exception that hGH Y42A/Q46A/G120R represents data from a single protein preparation). Errors are given as standard deviations. <sup>b</sup> Changes in free energy are calculated from  $-RT \ln (1/K_d)$  (Table 2). <sup>c</sup> Linear regression of the temperature dependence of  $\Delta H$  yielded  $\Delta C_p$  values as shown in Figure 5. Uncertainties are reported as the standard deviation of linear regression parameters.

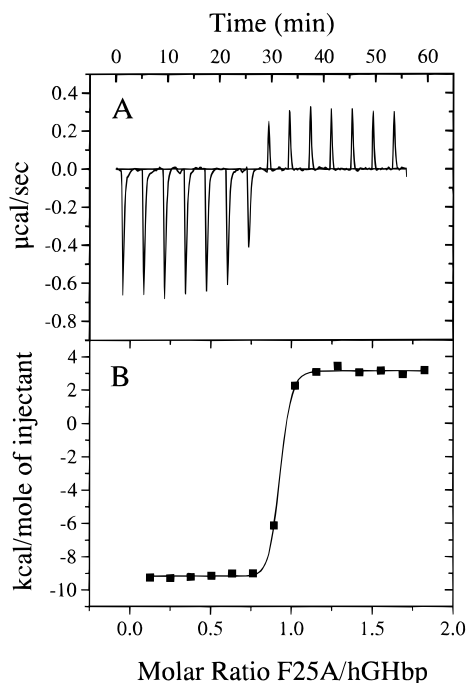


FIGURE 4: Titration calorimetry. (Panel A) Shown is a typical titration calorimetry scan for F25A/G120R binding to the hGHbp. Fourteen consecutive injections (duration time = 5 s and interval time = 240 s) of the variant hormone ( $8.7 \mu\text{L}$ ;  $257 \mu\text{M}$ ) were added to the stirred hGHbp solution ( $1.394 \text{ mL}$ ;  $13.6 \mu\text{M}$ ) at  $26.2$  °C. Negative and positive peaks represent the heat release upon binding and the heat absorbed upon ligand dilution, respectively. (Panel B) Integration of the peaks yields a  $\Delta H$  per injection. Shown is a plot of heats of reaction versus the ratio of ligand–receptor following injection. The solid line shows the best fit obtained by least-squares regression using a one-site model; this analysis gave a determined stoichiometry value of 0.93.

binding to the hGHbp at  $26$  °C. The  $\Delta S$  values were calculated using the standard thermodynamic relationship,  $\Delta G = \Delta H - T\Delta S$  (where  $T$  is absolute temperature).

A typical isothermal titration is shown in Figure 4A. The negative peaks produced when less than saturating amounts of hGH were titrated into the calorimetry cell indicate an exothermic process upon binding to the hGHbp. After the addition of 1 equiv of the variant hormones (Figure 4), injections produced positive peaks since, in this case, ligand dilution is an endothermic process. As expected, the stoichiometry of binding calculated for each of the binding reactions was close to 1.0 (data not shown), since all the variants contained the G120R mutation. To calculate the  $\Delta H_{\text{assoc}}$ , the average heat of ligand dilution was subtracted from the heat released for each subsaturating hGH injection to yield the heat of binding:  $\Delta H_{\text{assoc}} = \Delta H_{\text{total}} - \Delta H_{\text{dilution}}$ . The  $\Delta H_{\text{dilution}}$  was virtually the same for each hGH variant solution (data not shown).

The thermodynamic parameters for these binding reactions were characterized by large negative enthalpies of binding (Table 3). For the G120R mutant roughly 80% of the  $\Delta G_{\text{assoc}}$  can be attributed to the  $\Delta H_{\text{assoc}}$ . The triple-alanine mutant had an even more negative heat change than G120R ( $-12.2$  kcal/mol versus  $-9.4$  kcal/mol, respectively). To identify the source of the greater enthalpy change, we dissected the triple-alanine mutant into the two components, F25A and Y42A/Q46A. The F25A variant had virtually the same  $\Delta H_{\text{assoc}}$  as the triple-alanine mutant, whereas the Y42A/Q46A had the same  $\Delta H_{\text{assoc}}$  as the G120R alone. The greater  $\Delta H_{\text{assoc}}$  for the F25A mutation could result from several factors; one possibility is that in the wild-type binding event desolvation of the phenyl ring causes the release of ordered solvent (Gill et al., 1976), and this contributes unfavorably to the enthalpy of binding. Therefore, the absence of the phenyl ring in the F25A mutant removes the endothermic process of losing ordered water molecules to bulk solvent.

The less favorable enthalpy of binding for the G120R interaction compared to the F25A interaction is in agreement with solvation enthalpies of benzene derived from small molecule transfer experiments by Gill et al. (1976). However, this trend is in contrast to several other small molecule transfer studies (Tanford, 1980; Murphy & Gill, 1991). For example, Murphy and Gill (1991) used the dissolution of cyclic peptides to predict that desolvation of a phenyl group would yield a  $-1.1$  kcal/mol contribution to the enthalpy of binding. Such inconsistencies further support the notion that thermodynamic relationships derived from small model compounds may not accurately represent intermolecular side chain interactions in the context of large protein–protein interfaces. Effects of mutations at interface residues on enthalpy and entropy of binding may depend on the microscopic environments of the side chains in both the free and bound states.

Using an analysis described by Murphy and Freire (1992), a comparison can be made between the measured  $\Delta H_{\text{assoc}}$  and the calculated  $\Delta H_{\text{assoc}}$ . From the calculation of polar and nonpolar surface area buried ( $\Delta A_p$  and  $\Delta A_{np}$ , respectively) for both the G120R and triple-alanine 1:1 complexes,<sup>2</sup> the contribution to  $\Delta C_p$  can be estimated with relationships as shown in eq 4. Thus, both the nonpolar and polar contributions to  $\Delta C_p$  can be used in the equations (Murphy & Freire, 1992)

<sup>2</sup> The structure of the 1:1 hGH G120R–hGHbp complex was solved at  $2.6$  Å; inclusion of water molecules in combination with positional refinement resulted in a final  $R$ -value of 0.187 (A. De Vos and M. Ultsch, unpublished results). From both crystal structures, calculation of the decrease in solvent-accessible surface area upon binding was made with the use of the Lee and Richards algorithm (Lee & Richards, 1971) using a probe radius of  $1.4$  Å.

$$\Delta H_{np} = \Delta C_{p,np}(T - T_H^\dagger) \quad (1)$$

$$\Delta H_p = \Delta H^\dagger(\Delta A_p) + \Delta C_{p,p}(T - T_H^\dagger) \quad (2)$$

to yield the nonpolar enthalpy change,  $\Delta H_{np}$ , and the polar enthalpy change,  $\Delta H_p$ , where the reference temperature  $T_H^\dagger = 100.5^\circ\text{C}$ , and the residual enthalpy change  $\Delta H^\dagger = 35 \text{ cal}/(\text{mol}\cdot\text{\AA}^2)$ .

Using the structural parameters to calculate the  $\Delta H_{\text{assoc}}$  for each reaction at  $26^\circ\text{C}$  yields  $-12.5 \text{ kcal/mol}$  for the G120R–hGHbp complex and  $-12.1 \text{ kcal/mol}$  for the triple-alanine–hGHbp complex. These calculated values compare rather favorably with the measured values of  $-9.4 \pm 0.3 \text{ kcal/mol}$  for G120R and  $-12.2 \pm 0.7 \text{ kcal/mol}$  for triple-alanine binding at  $26^\circ\text{C}$ . However, the discrepancy between the calculated and the measured  $\Delta H_{\text{assoc}}$  values decreases (from approximately 25% difference at  $26^\circ\text{C}$  to approximately 8% difference at  $38^\circ\text{C}$ ) with an increase in temperature for the G120R reaction, and the discrepancy increases (from approximately 1% difference at  $26^\circ\text{C}$  to approximately 33% difference at  $38^\circ\text{C}$ ) with an increase in temperature for the triple-alanine reaction. It should be noted that calculations based on the triple-alanine–hGHbp 1:1 complex are estimates due to a significant degree of disorder in the hGH minihelical region of the structure.

Given the more negative enthalpy change for binding of the F25A-containing hormones, to maintain the same free energy of binding, the entropic terms were correspondingly less favorable compared to the G120R hGH–hGHbp and Y42A/Q46A/G120R hGH–hGHbp interactions (Table 3). Overall, the trend to less favorable entropic contributions upon removal of F25 suggests that desolvation of the exposed phenylalanine occurs upon binding. In some respects, it is somewhat surprising that the Y42A/Q46A binding events did not demonstrate a substantially more favorable entropy term compared to the G120R reaction. Since the crystal structure shows that the minihelical region is apparently disordered in the mutant complex, it might be expected that there would be less of a configurational entropic barrier to binding for Y42A/Q46A. However, comparison of the 1:1 complex structure with structures of the free triple-alanine mutant and G120R is necessary for further elaboration on this point. Even though electron density was not well-defined in this region of the complex, the data cannot give an indication of the degree of disorder.

The entropic contribution to binding is at least four times smaller than the enthalpy of binding for all the mutants. In general, given the large surface area involved at this interface, one may have expected that a significant number of water molecules would be displaced upon association to result in a much more favorable entropy term than that observed. However, the total entropic contribution to binding can be subdivided into a number of components (such as solvent, rotational, vibrational, and conformational effects) (Sturtevant, 1977); therefore, it is difficult to predict what the overall entropic contribution to binding would be on the basis of the structural information of the 1:1 complex. To clarify the relative solvation between free and bound states, structural analysis of the free components is necessary.

*Heat Capacity Measurements Suggest That Binding Is Driven by Hydrophobic Interactions That Become Stronger in the Triple-Alanine Mutant.* The heat capacity change,

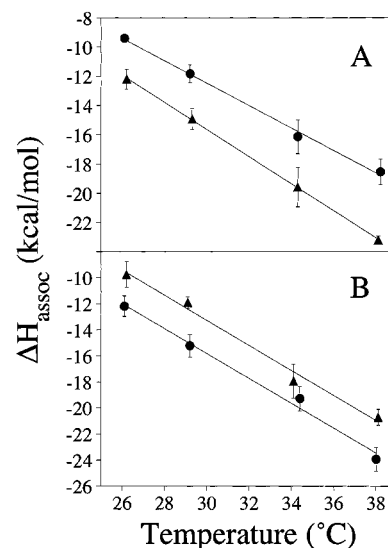


FIGURE 5: Temperature dependence of  $\Delta H$  for hGH variant–hGHbp binding. (Panel A) The change in  $\Delta H_{\text{assoc}}$  with temperature is shown for the G120R (circles) F25A/Y42A/Q46A/G120R (triangles) variants. (Panel B) Shown is the change in  $\Delta H_{\text{assoc}}$  for the F25A/G120R (circles) and Y42A/Q46A/G120R (triangles) variants. Error bars represent the standard deviation for multiple injections (ranging between 2 and 13). The slope of the solid line gives the heat capacity change ( $\Delta C_p$ ) as summarized in Table 3.

$\Delta C_p$ , upon protein–protein interaction has previously been related to the nonpolar surface area buried upon protein folding or protein–protein association (Varadarajan et al., 1992; Spolar & Record, 1994). Generally, large negative heat capacities have been found to correspond to exclusion of highly ordered water molecules from exposed hydrophobic areas on unfolded proteins or free unassociated ligands (Jelesarov & Bosshard, 1994; Spolar & Record, 1994; Livingstone et al., 1991). Hydrophobic interactions tend to generate negative contributions whereas electrostatic interactions generate positive changes in heat capacity of binding (Sturtevant, 1977; Tanford, 1980; Makhatadze & Privalov, 1990; Livingstone et al., 1991). To calculate the change in heat capacity, we measured the enthalpy of binding as a function of temperature and applied the relationship (Privalov & Gill, 1988):

$$\Delta H(T) = \Delta H(T_0) + \Delta C_p(T - T_0) \quad (3)$$

This assumes that  $\Delta C_p$  is temperature independent in the temperature range of the experiment. As shown in Figure 5,  $\Delta H$  as a function of temperature was linear for all four mutants between 26 and  $38^\circ\text{C}$  (Figure 5). For the G120R hGH–hGHbp interaction, the change in heat capacity was determined to be  $-767 \pm 34 \text{ cal}/(\text{mol}\cdot\text{K})$ . This large negative value for the change in heat capacity is similar to other values reported for protein–protein interactions (Varadarajan et al., 1992; Kelly et al., 1992; Spolar & Record, 1994; Hibbits et al., 1994).

In all three hGH variants tested, the  $\Delta C_p$  values were significantly more negative than for the wild-type site 1 interaction (Table 3). This result was somewhat unexpected given the fact that the F25A and the Y42A mutations remove hydrophobic side chains that are substantially buried at the interface. Another interesting aspect of these measurements is that the mutational effects on the  $\Delta C_p$  values were not additive for the component mutations whereas effects on the

enthalpy and entropy of binding (at 26 °C) were reasonably additive. At present, there is no satisfying explanation for this observation. Preliminary temperature denaturation experiments by differential scanning calorimetry indicate that the  $T_m$  values for unfolding for both hGH ( $T_m \approx 75$  °C) and hGHbp ( $T_m \approx 49$  °C) are above the maximum temperature used for  $\Delta C_p$  determination by isothermal titration calorimetry (38 °C). Therefore, the  $\Delta C_p$  measurements are not affected by protein folding upon binding.

Comparison of the change in nonpolar surface area buried between the wild-type hGH–hGHbp and F25A hGH–hGHbp using the crystal structures of the G120R and F25A/Y42A/Q46A 1:1 complexes with hGHbp shows that approximately  $37 \text{ \AA}^2$  ( $\Delta\Delta A_{np}$ ) more nonpolar area is buried with a phenylalanine at position 25 versus an alanine. This area value was determined by calculating the decrease in solvent-accessible area (Lee & Richards, 1971) for F25 and F25A in the respective structures and taking the difference in areas to yield  $\Delta\Delta A_{np}$ . Using the relationship

$$\Delta\Delta C_p = (0.45 \pm 0.02)\Delta\Delta A_{np} - (0.26 \pm 0.03)\Delta\Delta A_p \quad \text{cal}/(\text{mol}\cdot\text{K}) \quad (4)$$

(Murphy et al., 1992) the expected  $\Delta\Delta C_p$  can be determined from the  $\Delta\Delta A_{np}$  value derived from the crystal structures of the two complexes. From Table 3, the experimentally determined change in heat capacity difference can be calculated as  $\Delta\Delta C_p(\text{exptl}) = \Delta C_p(\text{wt}) - \Delta C_p(\text{mut}) = +189 \text{ cal}/(\text{mol}\cdot\text{K})$ . Comparison of this value to the calculated value using  $\Delta\Delta A_{np}$  and eq 4 [ $\Delta\Delta C_p(\text{calc}) = +16.7 \text{ cal}/(\text{mol}\cdot\text{K})$ ] shows that the magnitude of the experimentally determined value does not compare well to the value obtained from structural parameters and the relationship (eq 4) derived from small molecule transfer studies. Additionally, the  $\Delta C_p(\text{exptl})$  [ $-767 \text{ cal}/(\text{mol}\cdot\text{K})$ ; Table 3] and the  $\Delta C_p(\text{calc})$  [ $-364 \text{ cal}/(\text{mol}\cdot\text{K})$ ;  $\Delta A_{np} = -1465 \text{ \AA}^2$  and  $\Delta A_p = -1134 \text{ \AA}^2$ ; De Vos and Ultsch, in preparation] for the G120R hGH–hGHbp interaction and the  $\Delta C_p(\text{exptl})$  [ $-927 \text{ cal}/(\text{mol}\cdot\text{K})$ ; Table 3] and the  $\Delta C_p(\text{calc})$  [ $-295 \text{ cal}/(\text{mol}\cdot\text{K})$ ;  $\Delta A_{np} = -1218 \text{ \AA}^2$  and  $\Delta A_p = -974 \text{ \AA}^2$ ] for the triple-alanine–hGHbp interaction do not correlate very well. Determination of  $\Delta C_p(\text{calc})$  from area buried data using the relationship of Spolar and Record (1994) also yielded less negative  $\Delta C_p$  values compared to  $\Delta C_p(\text{exptl})$ . Similar discrepancies concerning  $\Delta C_p$  and surface area buried have also been reported for antibody–antigen interactions (Kelley & O'Connell, 1993) and S-peptide–S-protein interactions (Varadarajan et al., 1992). Although these apparent differences cannot be readily explained, they suggest that there are significant complicating factors involved in using small molecule transfer or dissolution-derived relationships to describe the effects of mutations of amino acids at a large protein–protein interface.

**Affinity-Inert Contacts for the hGHbp Can Still Be Functionally Important.** Although mutation of F25, Y42, and Q46 to alanine affects neither the affinity nor kinetics of binding to the hGH receptor, they may play other roles. hGH is a multifunctional hormone and binds to at least one other receptor, the prolactin receptor (Somers et al., 1994). In fact, the F25A mutation causes a 7-fold reduction in prolactin receptor binding (Cunningham & Wells, 1991). Thus, some of these affinity-inert residues for binding the hGHbp can still be important for binding other receptors or for preventing binding of other receptors. Furthermore, the

affinity inert polar residues may promote solubility of this interface where hydrophobic interactions tend to dominate the interaction.

## CONCLUSIONS

Not all contact residues at a protein–protein interface are critical for binding. Here, removal of at least 16% of the contact interface at site 1 in the hGH–hGHbp complex caused almost no change in the binding affinity or kinetics. While these mutations at the interface caused essentially no global structural change, the minihelix at the variant hGH–hGHbp interface is partially disordered. These studies support the notion that massive cumulative reductions in some molecular contacts at a protein–protein interface can be tolerated with minimal change in affinity. In another recent example, a total of 16 alanine mutations that encircled five functionally critical residues for binding hGH to a monoclonal antibody could be simultaneously introduced with little effect on binding affinity (Jin & Wells, 1994). These and other experiments (Kelley & O'Connell, 1993; Cunningham & Wells, 1993; Niu et al., 1994; Clackson & Wells, 1995) suggest there are hot spots of binding energy at protein–protein interfaces. We have suggested such sites may be targets for rational drug design (Clackson & Wells, 1995).

Although mutations at these inert contact residues caused little free energy change, there were sometimes compensating changes in the enthalpy and entropy of binding. In fact, these component thermodynamic parameters appeared more sensitive to changes in contact residues than the overall free energy. Compensation in enthalpy–entropy terms has been reported previously for protein–protein interactions upon solvent isotopic substitution (Chervenak & Toone, 1994), with temperature change (Hibbits et al., 1994; Kelley et al., 1992) and amino acid substitution (Brummell et al., 1993); enthalpy–entropy compensation has also been observed for protein–carbohydrate (Brummell et al., 1993) and for protein–haptens (Herron et al., 1986) interactions. Detailed interpretation of the changes in the enthalpy and entropy of binding is confounded by the absence of a detailed understanding of solvent structure as well as structures of the unbound components.

The negative heat capacity measurements are entirely consistent with previous mutational studies, indicating that hydrophobic forces dominate the affinity for this interaction (Clackson & Wells, 1995). However, the predicted heat capacity changes based on changes in area buried at the interface were discrepant from those measured for any of the mutants. These results suggest that small molecule model systems may not be adequate for mimicking the role of hydrophobic side chains in the context of a protein–protein interface (Murphy & Gill, 1989; Spolar et al., 1992). Furthermore, the effects on  $\Delta C_p$  were not additive whereas the other thermodynamic parameters (at 26 °C) appeared additive. Prediction of thermodynamic parameters from structural data such as buried surface area is central to understanding the molecular basis for protein–protein interaction (Chothia & Janin, 1975; Horton & Lewis, 1992; Vakser & Aflalo, 1994). However, the structural results in conjunction with the thermodynamic measurements presented here emphasize the inherent difficulty in predicting such relationships.

Finally, these studies show various ways mutations at protein–protein interfaces can be accommodated. For the F25A, a simple cavity was produced which we presume to be solvent filled. For the Y42A/Q46A mutations, some apparent disorder was introduced into a previously well-defined helical segment. It is noteworthy, but perhaps only coincidental, that these structural changes occurred in regions that are prone to flexibility. This result suggests the possibility that regions that are more dynamic at this interface are ones that are less important for affinity.

## ACKNOWLEDGMENT

We thank Beth Gillece-Castro and Jim Bourrell for mass spectrometry, Allen Padua for quantitative amino acid analysis, Han Chen and Brad Snedecor for fermentation, David Wood and Kerrie Andow for help with graphics, and the oligonucleotide synthesis group at Genentech.

## REFERENCES

- Abdel-Meguid, S. S., Shieh, H.-S., Smith, W. W., Dayringer, H. E., Vieland, B. N., & Bente, L. A. (1987) *Proc. Natl. Acad. Sci. U.S.A.* **84**, 6434–6437.
- Brummell, D. A., Sharma, V. P., Anand, N. N., Bilous, D., Dubuc, G., Michniewicz, J., MacKenzie, C. R., Sadowaka, J., Sigurskjold, B. W., Sinnott, B., Young, N. M., Bundle, D. R., & Narang, S. A. (1993) *Biochemistry* **32**, 1180–1187.
- Brünger, A. T. (1992) *X-PLOR Reference Manual*, Yale University Press, New Haven, CT.
- Chervenak, M. C., & Toone, E. J. (1994) *J. Am. Chem. Soc.* **116**, 10533–10539.
- Chothia, C., & Janin, J. (1975) *Nature* **256**, 705–708.
- Clackson, T., & Wells, J. A. (1995) *Science* **267**, 383–386.
- Cunningham, B. C., & Wells, J. A. (1989) *Science* **244**, 1081–1085.
- Cunningham, B. C., & Wells, J. A. (1991) *Proc. Natl. Acad. Sci. U.S.A.* **88**, 3407–3411.
- Cunningham, B. C., & Wells, J. A. (1993) *J. Mol. Biol.* **234**, 554–563.
- De Vos, A. M., Ultsch, M., & Kossiakoff, A. A. (1992) *Science* **255**, 306–312.
- Engh, R. A., & Huber, R. (1991) *Acta Crystallogr. A* **47**, 392–400.
- Ferrin, T. E., Huang, C. L., Jarvis, L. E., & Langridge, R. (1988) *J. Mol. Graphics* **6**, 13–27.
- Fuh, G., Cunningham, B. C., Fukunaga, R., Nagata, S., Goeddel, D. V., & Wells, J. A. (1992) *Science* **256**, 1677–1680.
- Gill, S. J., Nichols, N. F., & Wadsö, I. (1976) *J. Chem. Thermodyn.* **8**, 445–452.
- Herron, J. N., Kranz, D. M., Jameson, D. M., & Voss, E. W. (1986) *Biochemistry* **25**, 4602–4609.
- Hibbits, K. A., Gill, D. S., & Willson, R. C. (1994) *Biochemistry* **33**, 3584–3590.
- Horton, N., & Lewis, M. (1992) *Protein Sci.* **1**, 169–181.
- Jelesarov, I., & Bosshard, H. R. (1994) *Biochemistry* **33**, 13321–13328.
- Jin, L., & Wells, J. A. (1994) *Protein Sci.* **3**, 2351–2357.
- Jones, A. T. (1978) *J. Appl. Crystallogr.* **11**, 268–272.
- Kabsch, W. (1988) *J. Appl. Crystallogr.* **21**, 916–934.
- Kelley, R. F., & O'Connell, M. P. (1993) *Biochemistry* **32**, 6828–6835.
- Kelley, R. F., O'Connell, M. P., Carter, P., Presta, L., Eigenbrot, C., Covarrubias, M., Snedecor, B., Bourell, J. H., & Vetterlein, D. (1992) *Biochemistry* **31**, 5434–5441.
- Lee, B. K., & Richards, F. M. (1971) *J. Mol. Biol.* **55**, 379–400.
- Livingstone, J. R., Spolar, R. S., & Record, M. T. (1991) *Biochemistry* **30**, 4237–4244.
- Lowman, H. B., & Wells, J. A. (1993) *J. Mol. Biol.* **234**, 564–578.
- Makhatadze, G. I., & Privalov, P. L. (1990) *J. Mol. Biol.* **213**, 375–384.
- Murphy, K. P., & Gill, S. J. (1989) *J. Chem. Thermodynam.* **21**, 903–913.
- Murphy, K. P., & Gill, S. J. (1991) *J. Mol. Biol.* **222**, 699–709.
- Murphy, K. P., & Freire, E. (1992) *Adv. Protein Chem.* **42**, 313–361.
- Murphy, K. P., Bhakuni, V., Xie, D., & Freire, E. (1992) *J. Mol. Biol.* **227**, 293–306.
- Nui, W., Zhou, Y., Dong, Q., Ebright, Y. W., & Ebright, R. H. (1994) *J. Mol. Biol.* **243**, 595–602.
- Privalov, P. L., & Gill, S. J. (1988) *Adv. Protein Chem.* **39**, 191–234.
- Somers, W., Ultsch, M., De Vos, A. M., & Kossiakoff, A. A. (1994) *Nature* **372**, 478–481.
- Spolar, R. S., & Record, M. T. (1994) *Science* **263**, 777–784.
- Sturtevant, J. M. (1977) *Proc. Natl. Acad. Sci. U.S.A.* **74**, 2236–2240.
- Tanford, C. (1980) in *The Hydrophobic Effect*, John Wiley & Sons, New York.
- Ultsch, M., & De Vos, A. M. (1993) *J. Mol. Biol.* **231**, 1133–1136.
- Ultsch, M., Somers, W., Kossiakoff, A. A., & De Vos, A. M. (1994) *J. Mol. Biol.* **236**, 289–299.
- Vakser, I. A., & Aflalo, C. (1994) *Proteins* **20**, 320–329.
- Varadarajan, R., Connelly, P. R., Sturtevant, J. M., & Richards, F. M. (1992) *Biochemistry* **31**, 1421–1426.
- Wells, J. A., & De Vos, A. M. (1996) *Annu. Rev. Biochem.* **65**, 609–634.
- Wiseman, T., Williston, S., Brandts, J. F., & Lin, L.-N. (1989) *Anal. Biochem.* **179**, 131–137.

BI960513B